Effect of NdB6 addition on densification and properties of ZrB2

Sonber, J.K.; Murthy, T.S.R.Ch; Sairam, K.; Chakravartty, J.K.

DOI:
10.13168/cs.2016.0006

Ceramics-Silikáty 60 (2), 41-47 (2016)
journal webpage: www.ceramics-silikaty.cz doi: 10.13168/cs.2016.0006

EFFECT OF NdB_6 ADDITION ON DENSIFICATION AND PROPERTIES OF ZrB_2

#J. K. SONBER, T. S. R. CH. MURTHY, K. SAIRAM AND J. K. CHAKRAVARTTY

Materials Group, Bhabha Atomic Research Centre, Mumbai, India – 400 085

#E-mail: jitendra@barc.gov.in

Submitted November 9, 2015; accepted February 7, 2016

Keywords: ZrB_2, Densification, NdB_6, Hot pressing, Oxidation

This paper reports on the effect of NdB_6 addition on densification and properties of ZrB_2. NdB_6 powder (2.5, 5 and 10 wt. %) was added to ZrB_2 powder and consolidated by hot pressing. It was found that NdB_6 addition assisted in densification of ZrB_2 at lower hot pressing temperature of 1750°C. Formation of solid solution was observed at the interface of ZrB_2 and NdB_6 phases. Hardness was found to be slightly increased by 2.5 wt. % NdB_6 addition but decreased by 5 and 10 % NdB_6 addition. Fracture toughness of composite is found to be higher than the monolithic ceramic. It was found that composite samples have excellent oxidation resistance at 900°C in air.

INTRODUCTION

Zirconium diboride has attracted extensive attention due to excellent combination of properties as high melting point, high hardness, high thermal and electrical conductivity, high temperature strength and thermal shock resistance [1-3]. It is considered a potential material for hypersonic flight, atmospheric re-entry and rocket propulsion [1, 4]. It is a highly promising candidate for the leading edges of future re-entry vehicles which will have sharp edges for better flight performance [1, 3-5]. It is expected to be used for electrode application in Hall -Heroult cell and electric discharge machining due to its good electrical conductivity [6-8]. It is also considered a suitable material for neutron absorber in nuclear reactors. [9-10]

Despite of attractive properties of ZrB_2, its applicability is limited due to its poor sinterability and low fracture toughness. Poor sinterability of ZrB_2 is due to low self diffusivity and strong covalent bonding. Dense ZrB_2 shapes can be fabricated by hot pressing or spark plasma sintering at high temperatures (~ 1900ºC) [1, 11]. Previous studies have shown improved sintering behavior and properties by the addition of second phase [12-15]. Carbon and carbide additions were reported to accelerate densification by reacting with the oxide layer present in the surface of ZrB_2 particles [16-20]. Addition of silicides such as $TiSi_2$, $ZrSi_2$, $CrSi_2$ and $TaSi_2$ improved the densification of ZrB_2 by formation of liquid phases during sintering. [21-23]. Metallic addition such as Ni is also reported to improve the densification by liquid phase sintering [19].Though, metal and silicide additions lower the hot pressing temperature, they are also expected to deteriorate the mechanical properties.

Rare earth hexaborides are remarkable materials due to their refractory nature and good physical properties such as high thermal and electrical conductivity. Moreover these hexabrides are expected to form solid solution with ZrB_2 and assist in densification. As per author's knowledge there is no literature on the application of NdB_6 as sinter additive for ZrB_2. NdB_6 has high melting point and thus would be a promising additive for high temperature application. The purpose of the present study is to elucidate the effect of NdB_6 on processing and properties of ZrB_2. Salient properties of ZrB_2 and NdB_6 are given in Table 1.

Table 1. Salient properties of ZrB_2 and NdB_6*.

Property	ZrB_2	NdB_6
Crystal structure	Hexagonal	Cubic
Density	6.1	4.95
Melting point	3245	2610
Thermal expansion coefficient ($°C^{-1}$)	5.9×10^{-6}	7.3×10^{-6}
Thermal conductivity	57.9	47
Elastic modulus (GPa)	489	–
Hardness (GPa)	23.91	24.9

EXPERIMENTAL

Starting material

In house prepared ZrB_2 (D_{50}: 2.7 μm, 'C': 0.6 wt. %, 'O': 0.5 wt. %) and NdB_6 (D_{50}: 2.5 μm, 'C': 0.8, 'O': 0.7 wt. %) powders were used as starting materials. Preparation details of ZrB_2 powder is presented elsewhere [24]. NdB_6 was prepared by boron carbide reduction of Nd_2O_3. Mean particle diameters of starting powders were measured by laser diffraction method (CILAS PSA 1064L). Figure 1 presents the XRD pattern of the starting powders. Figure 2 presents the SEM images of powder which show that both ZrB_2 and NdB_6 particles are equiaxular and in the range of 2 - 4 μm. No agglomerations were observed in the starting powders.

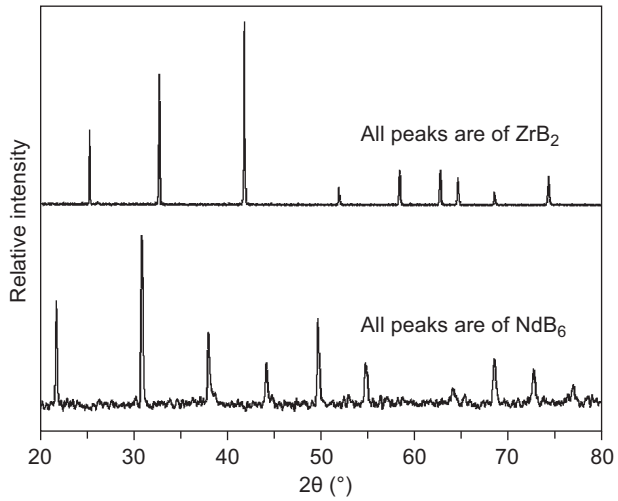

Figure 1. XRD pattern of starting materials: a) ZrB_2, b) NdB_6.

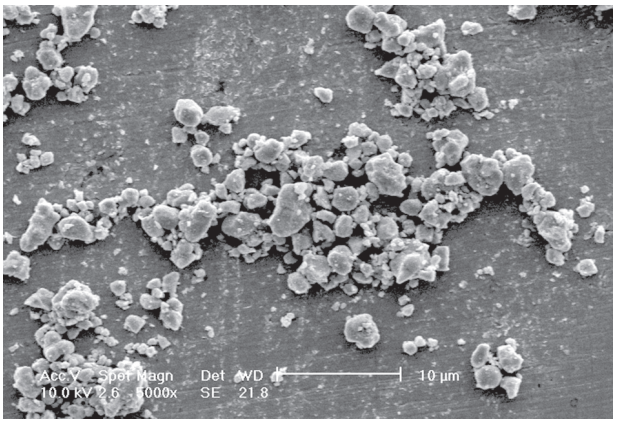

a) ZrB_2

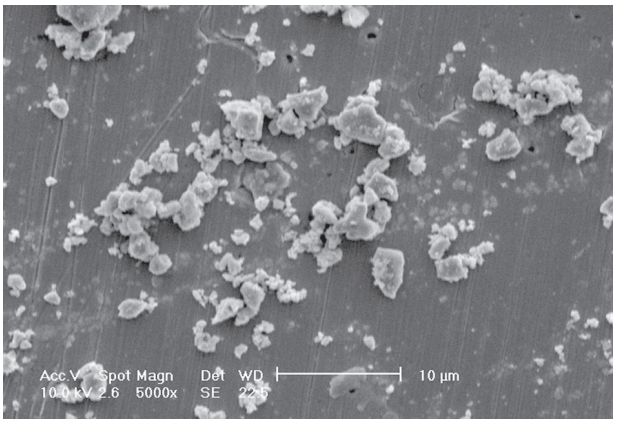

b) NdB_6

Figure 2. SEM image of starting powders: a) ZrB_2, b) NdB_6.

Densification and characterization

For densification, weighed quantities of fine zirconium diboride and neodymium hexaboride were mixed thoroughly using a motorized mortar and pestle in dry condition for 1 h to obtain samples of different compositions. The powders were then loaded in a high density graphite die (12 mm diameter) and hot pressed at a temperature of 1750°C under a pressure of 35 MPa for 2 hour in a high vacuum (1×10^{-5} mbar) chamber. The pellets were ejected from the die after cooling and the density measured by liquid displacement method. Densified samples were polished to mirror finish using diamond powder of various grades from 15 to 0.25 μm in an auto polisher (laboforce-3, Struers). Microhardness was measured for polished samples under a load of 100 g and dwell time of 10 s. The indentation fracture toughness (K_{IC}) data were evaluated by crack length measurement of the crack pattern formed around Vickers indents (using 10 Kg load), adopting the model formulation proposed by Anstis et al. [25], $K_{IC} = 0.016(E/H)^{1/2}P/c^{3/2}$, where E is the Young's modulus, H the Vickers's hardness, P the applied indentation load, and c the half crack length. Young's moduli (E) of the samples were measured by ultrasonic method as per ASTM C1419 procedure. The reported value of hardness and fracture toughness are the average of five measured values. Polished and fractured surfaces of dense pellets were analyzed by scanning electron microscope and Energy dispersive spectroscopy (EDS).

Oxidation

Oxidation study of the composite was carried out at a temperature of 900°C. Hot pressed pellet of diameter 12 mm was cut into thin slice of 3 mm thickness. All the surfaces of the cut sample were polished with emery papers (1/0, 2/0, 3/0, 4/0) and finally with diamond paste up to 1 μm finish. Oxidation tests were conducted in a resistance heated furnace. In order to avoid oxidation during heating, the sample was directly inserted into the furnace on reaching the required temperature. Samples were placed in an alumina crucible kept into the furnace. The samples were oxidized for different time intervals (0.5, 1, 2, 4, 8, 16, 32 and 64 h) at the set temperature of 900°C. The samples were carefully weighed before and after exposure, to determine the weight change during the oxidation process. The morphology and nature of oxide layer was understood by observing the surface in a scanning electron microscope (SEM).

RESULTS AND DISCUSSION

Densification and characterization

Effect of NdB_6 addition on densification and properties were studied. Hot pressing conditions, relative densities, hardness and fracture toughness obtained for the ZrB_2 composites are presented in Table.2.

It was found that addition of 2.5 wt. % NdB_6 resulted in densification of 99.3 % ρ_{th} at a temperature of 1750°C and a pressure of 35 MPa. Under identical hot pressing conditions, a density of 96.5 % and 95.4 % TD was obtained in composites with 5 % and 10 % NdB_6 respectively. In case of monolithic ZrB_2, a near full

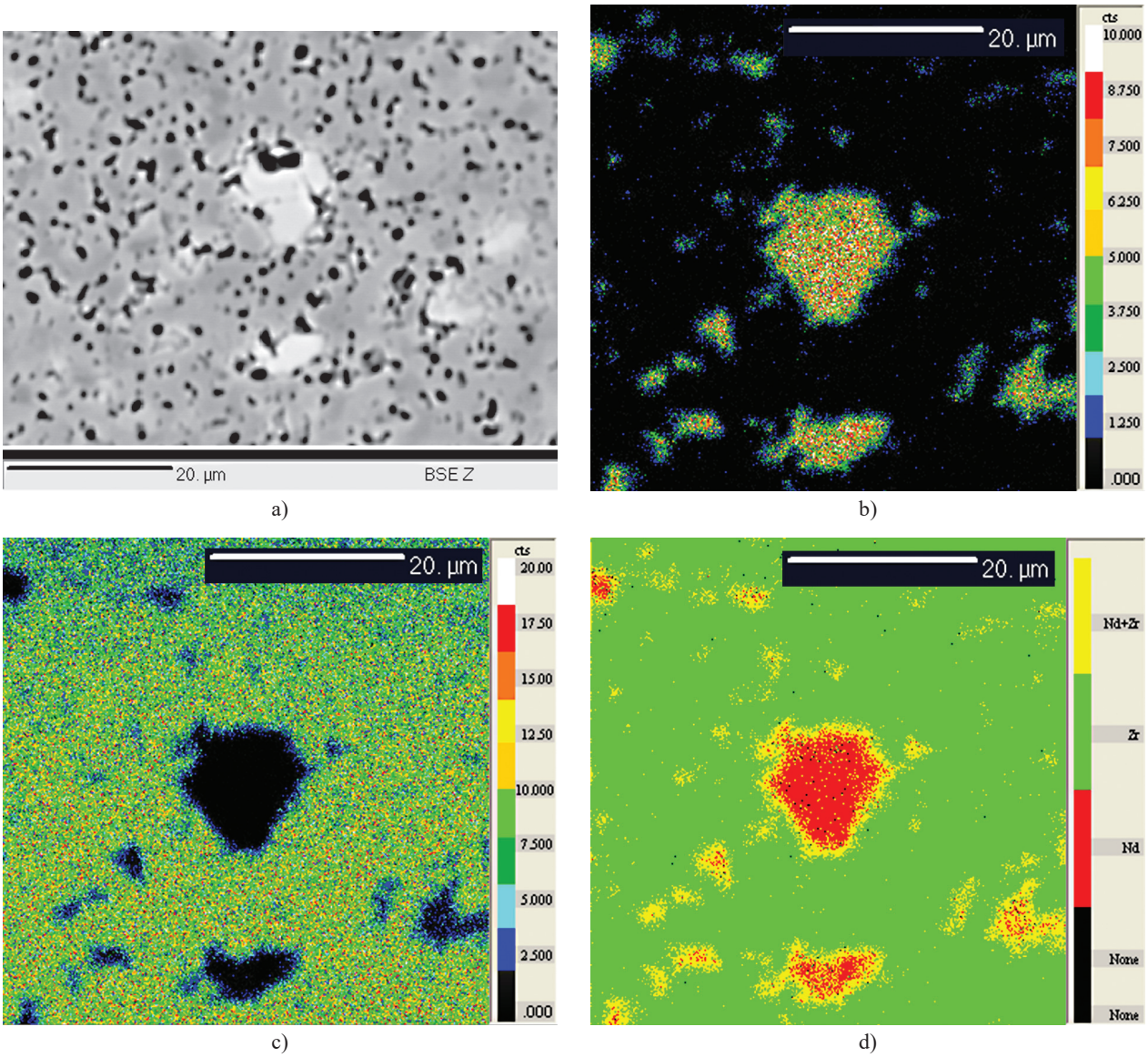

Figure 3. a) Back scattered image of ZrB_2 + 10 % NdB_6; b) Distribution of Nd; c) Distribution of Zr; d) Overlay of Zr and Nd distribution.

Table 2. Hot pressing conditions and properties of the ZrB_2 composites.

Sample	Temp. (°C)	Pressure (MPa)	Density (%)	Hardness (GPa) (100 gm)	K_{IC} ($MPa \cdot m^{1/2}$)
ZrB_2*	1850	35	99.8	23.91	3.31
ZrB_2	1750	35	80.3	–	-
ZrB_2 + 2.5 % NdB_6	1750	35	99.3	26.4 ± 2	4.25 ± 0.5
ZrB_2 + 5 % NdB_6	1750	35	96.5	21.7 ± 2	4.62 ± 0.5
ZrB_2 + 10 % NdB_6	1750	35	95.4	22.6 ± 2	4.74 ± 0.5

** Reference [20]*

density (99.8 % TD) was obtained at a higher temperature and pressure of 1850°C and 35 MPa [24]. In the present study, the hot pressing temperature was lower by 100°C. For the purpose of comparison, monolithic ZrB_2 was hot pressed at 1750°C and a density of merely 80.3 % TD is achieved. Addition of NdB_6 to ZrB_2 may result in the solid solution formation of ZrB_2 and NdB_6. On the formation of ZrB_2-NdB_6 solid solution, Nd takes Zr atom positions and boron occupies boron positions in the crystal structure. Due to large number of boron atoms from NdB_6, there will be generation of point defects in ZrB_2. The point defects are known to enhance the diffusional mass transfer and thus assist in densification at slightly reduced temperature. Formation of solid solution was confirmed by elemental analysis (EDS) of phases present in microstructure, which is discussed in the next paragraph.

Back scattered image of ZrB_2 + 10 % NdB_6 sample hot pressed at 1750°C is presented in Figure 3a. Distribution of Nd and Zr in the microstructure is presented in Figure 3b-d. It is obvious that the matrix is Zr rich and indeed it is ZrB_2. A second phase with white shades was found in the BSE image. Elemental mapping has revealed that the white shades are Nd rich and it must be NdB_6. Figure 3d presents the overlay distribution of Zr and Nd in the microstructure. In this image presence of three distinct pahses were noticed. Apart from ZrB_2 (green regions) and NdB_6 (red regions) there are yellow regions, which were analysed to contain both Zr and Nd. This suggested the formation of ZrB_2-NdB_6 solid solution. However, ZrB_2 and NdB_6 do not form complete solid solution and NdB_6 is also present as second phase in the composite as observed in the XRD pattern of the dense pellet of ZrB_2 + 10 % NdB_6 sample which is shown in Figure 4. It indicated the presence of crystalline ZrB_2 and NdB_6. One peak of ZrO_2 is also found in the XRD pattern which could be due to the oxygen pickup during mixing of ZrB_2 and NdB_6. Usually fine non oxide ceramics are associated with thin oxide layer as coating on the particles.

Comparison of other sinter additives from literature is discussed below. Guo et al. [26] have reported that addition of 5 % Re_2O_3 (Re = Y, Yb, La, Nd) to ZrB_2-20 % SiC results in > 99 % TD on hot pressing at 1900°C.

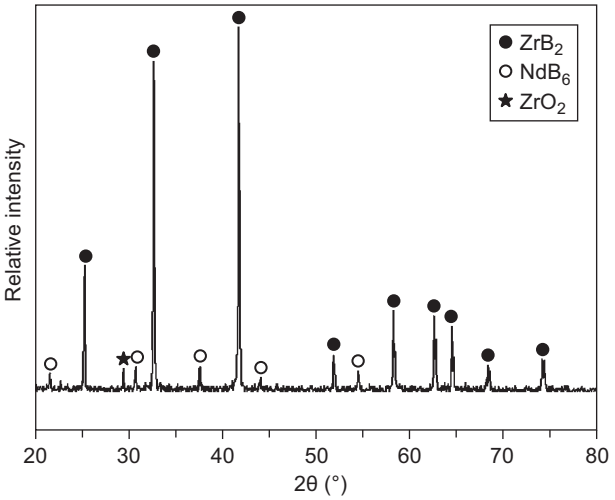

Figure 4. XRD pattern of Hot pressed ZrB_2 + 10 % NdB_6 sample.

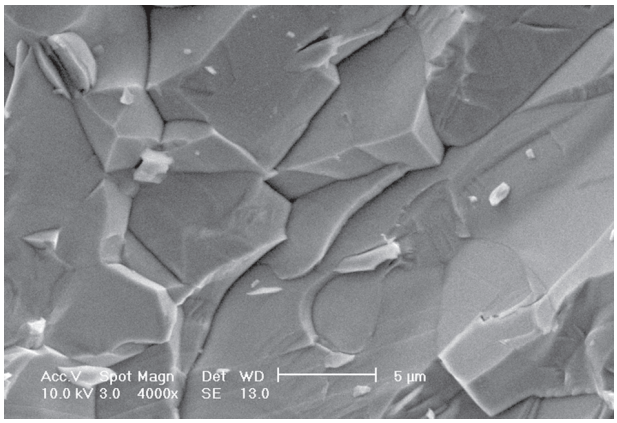

a)

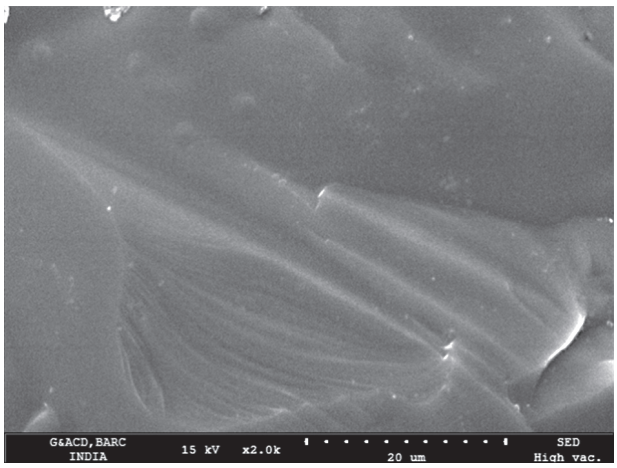

b)

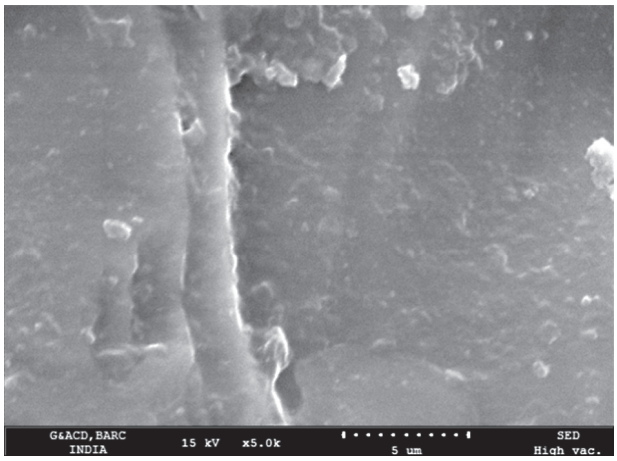

c)

Figure 5. Fractured surfaces of ZrB_2 composites: a) ZrB_2 + + 2.5 % NdB_6; b) ZrB_2 + 5 % NdB_6; c) ZrB_2 + 10 % NdB_6.

La_2O_3 and Nd_2O_3 react with surface oxides to form a liquid phase and promote densification of ZrB_2–SiC ceramics. Wang et al.[27] have reported that 10 % Mo addition gives a density of 98.9 % TD on hot pressing at 1950°C and 20 MPa.Zhu *et al* [28] have observed that addition of 3 - 10 % Al_2O_3 and Y_2O_3 and 20 % SiC_w to ZrB_2 gives a density > 97 % TD on hot pressing at 1800°C. From the above it is clear that addition of NdB_6 in the present investigation is found to be very effective in lowering the hot pressing temperature to 1750°C.

Mechanical properties and fractography

Variation in Vickers hardness and fracture toughness of ZrB_2 composites are presented in Table 2. Hardness of monolithic sample was measured as 23.9 ± 2 GPa [1], which increases to 26.4 ± 2 GPa with the addition of 2.5 wt. % NdB_6. The increase in hardness is attributed to the solid solution hardening by formation of ZrB_2––NdB_6 solid solution. On formation of solid solution the parent lattice gets strained and results in hardening of material. The hardness value of composite with 5 and 10 % NdB_6 addition was measured as 21.7 ± 2 and 22.6 ± 2 GPa respectively. The relatively lower hardness is due to the lower density of the hot pressed composite. Hardness of monolithic ZrB_2 has been reported to be in the range of 22 - 23 GPa [1, 2, 29]. Chamberlain et al. [29] have reported a hardness of 23 GPa for hot pressed ZrB_2. Silvestroni et al [30] have reported a hardness of 18.3 GPa for hot pressed ZrB_2 + 15 vol. % WSi_2. Hardness of ZrB_2 + EuB_6 composite has been reported in the range of 21 - 25 GPa [14].

Fracture surfaces of ZrB_2+NdB_6 composites are presented in Figure 5. It is obviously seen that the mode of fracture is transgranular in all the three composites. Fracture toughness of ZrB_2 + 2.5 % NdB_6 sample was measured as 4.25 MPa·$m^{1/2}$. With increased addition of NdB_6, fracture toughness increased gradually to 4.62 and 4.74 MPa·$m^{1/2}$ for composites containing 5 and 10 % NdB_6 respectively. The fracture toughness values obtained in the composite samples are found to be greater than the values reported for monolithic ZrB_2 in literature. Fracture toughness of monolithic ZrB_2 has been reported as 3.5 MPa·$m^{1/2}$[1]. Ran et al [31] have reported the enhancement of fracture toughness to 4.2 MPa·$m^{1/2}$ by 5 % SiC and 5 % ZrH_2 addition.

Oxidation study

The weight gain data obtained during oxidation at 900°C as a function of time for ZrB_2 + 2.5 % NdB_6, ZrB_2 + 5 % NdB_6 and ZrB_2 + 10 % NdB_6 samples are presented in Figure 6. All the three samples have shown continuous weight gain with time. On progress of oxidation it was observed that the rate of oxidation (slope of the curve) gets decreased. Figure 7 presents the rate of weight gain with time for ZrB_2 + 10 % NdB_6 sample. It shows sharp decrease in rate of oxidation just after initial oxidation. The decrease in rate of oxidation is credited to the formation of a protective layer. In the previous study [1], oxidation rate was found to be constant in case of monolithic ZrB_2. The enhancement of oxidation resistance of ZrB_2 by NdB_6 addition could be attributed to the formation of protective layer which could be a glassy layer based on boron, oxygen, Neodymium and zirconium.

Figure 8 presents the XRD pattern of oxidized surface. It shows the presence of ZrO_2 and Nd_2O_3 phase in crystalline form. One small peak of B_2O_3 is also present. Figure 9 presents the SEM microstructures of the oxidized surface. Presence of protective layer is evidently visible. Figure 10 presents the typical EDS pattern of oxide layer which indicates presence of Zr, Nd and O elements in the protective layer, which suggest the formation of Zr–Nd–B–O glassy phase which imparts resistance to oxidation by limiting the diffusion of oxygen through it. Presence of crystalline ZrO_2 and Nd_2O_3 phase

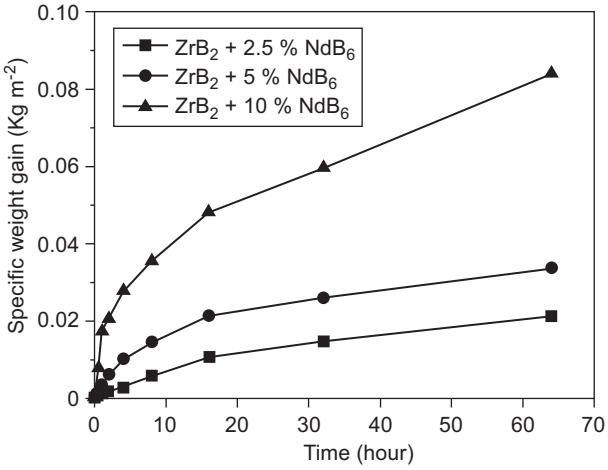

Figure 6. Specific weight gain vs time plot for ZrB_2 based composites after oxidation at 900°C for 64 hour.

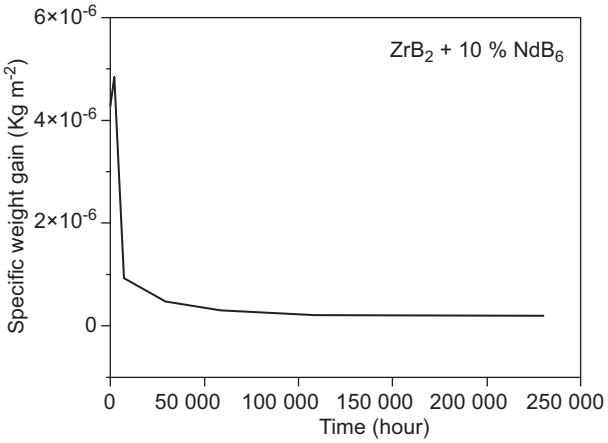

Figure 7. Rate of weight gain with time during oxidation of ZrB_2 + 10 % NdB_6 at 900°C in air.

in XRD pattern suggests that very fine zirconium oxide and neodymium oxide crystals could be present in the glassy layer.

The observations of other researchers on oxidation of ZrB_2 based material is discussed below. Sciti et al. [32] have found that on oxidation of ZrB_2 + 20 % $MoSi_2$ at 700°C, the extent of oxidation is very limited. Samples oxidized at temperature range 1200 - 1400°C was found to be covered by a continuous silica-rich glassy layer, in which small zirconia and/or zircon grains are embedded. Peng et al. [33] have studied the oxidation behaviour of ZrB_2 ceramic containing B_4C, SiC, TaB_2 and $TaSi_2$ by scanning thermogravimetry in the temperature range of 1150 to 1550°C. SiC additions improved oxidation resistance over a broadening range of temperatures. Tantalum additions to ZrB_2–B_4C–SiC in the form of TaB_2 and/or $TaSi_2$ increased oxidation resistance over the entire evaluated spectrum of temperatures. Dehdashti et al. [34] have studied the effect of tungsten addition on oxidation of ZrB_2. For pure ZrB_2, the protective liquid/glassy layer covering the surface as a result of oxidation was evaporated above 1500°C. For $(Zr,W)B_2$ specimens, the liquid/glassy layer was present after exposure up to 1600°C. Zhao et al [35] studied the effect of AlB_2 addition on oxidation of ZrB_2 at 1500°C. The oxidation tests revealed that the AlB_2 phase improved the oxidation resistance for the ZrB_2 based ceramics, owing to the Al–B–O liquid phase formed on the surface of the oxidized specimen, which slows down the oxygen transportation velocity.

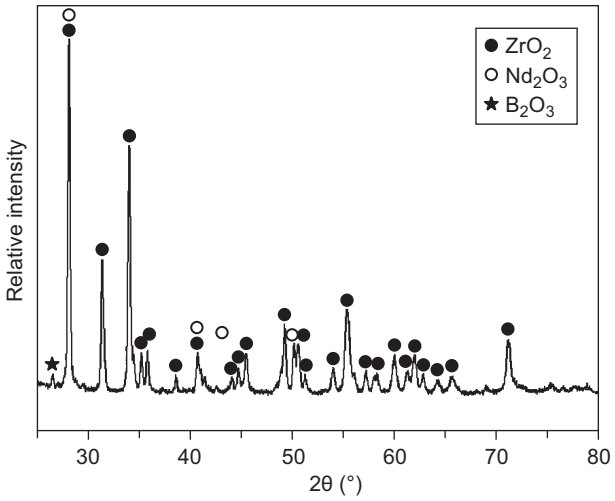

Figure 8. XRD pattern of ZrB_2 + 10 % NdB_6 sample after oxidation at 900°C for 64 hour.

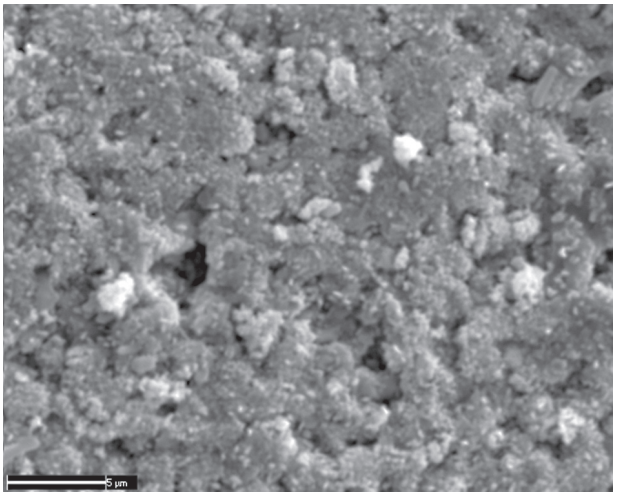

Figure 9. SEM image of ZrB_2 + 10 % NdB_6 composite after oxidation at 900°C for 64 hour.

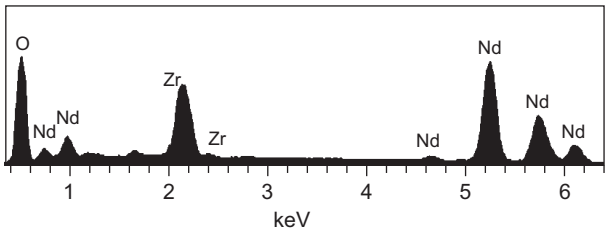

Figure 10. Typical EDS pattern of oxidized surface of ZrB_2 + 10 % NdB_6.

In this study, NdB_6 addition to ZrB_2 was found effective in improving the oxidation resistance at 900°C in ambient air.

CONCLUSION

Neodymium hexaboride was found to be an effective sintering aid for densification of ZrB_2. Addition of 2.5 % NdB_6 assisted in sintering and lowered the hot pressing temperature to 1750°C from 1850°C for monolithic ZrB_2. A mechanism was proposed to explain the reduction in sintering temperature. Formation of solid solution of ZrB_2 and NdB_6 was observed in microstructure analysis. As there is more number of boron atoms in NdB_6 there was formation of point defects in ZrB_2, which assisted in sintering. Addition of merely 2.5 % NdB_6 was found to enhance the hardness due to solid solution formation. Fracture toughness of the composite is found to be higher than that of monolithic ceramic. Oxidation resistance of ZrB_2 at the temperature of 900°C was improved by NdB_6 addition by the formation of protective oxide layer.

REFERENCE

1. Fahrenholtz W.G., Hilmas G.E., Talmy I.G., Zaykoski J.A. (2007): Refractory diborides of zirconium and hafnium. *Journal of the American Ceramic Society*, *90*(5), 1347-1364. doi:10.1111/j.1551-2916.2007.01583.x
2. Bauccio M.L. (1994). ASM Engineered Materials Reference book. ASM International, USA.
3. Upadhyay K., Yang J.M., Hoffman W.P. (1997): Materials for ultrahigh temperature structural application. *American Ceramic Society Bulletin*, *76*(12), 51-56.
4. Opeka M.M., Talmy I.G., Zaykoski J.A. (2004): Oxidation-based materials selection for 2000ºC + hypersonic aerosurfaces: Theoretical considerations and historical experience. *Journal of materials science*, *39*(19), 5887-5904. doi:10.1023/B:JMSC.0000041686.21788.77

5. Levine S.R., Opila E.J., Halbig M.C., Kiser J.D., Singh M., Salem J.A. (2002): Evaluation of ultra-high temperature ceramics for aeropropulsion use. *Journal of the European Ceramic Society, 22*, 2757-2767. doi:10.1016/S0955-2219(02)00140-1
6. Zaw H.M., Fuh J.Y.H., Nee A.Y.C., Lu L. (1999): For-mation of a new EDM electrode material using sintering techniques. *Journal of Materials Processing Technology*, *89*, 182-186. doi:10.1016/S0924-0136(99)00054-0
7. Khanra A.K., Sarkar B.R., Bhattacharya B., Pathak L.C., Godkhindi M.M. (2007): Performance of ZrB_2-Cu composite as an EDM electrode. *Journal of Materials Processing Technology*, *83*, 122-126. doi:10.1016/j.jmatprotec.2006.09.034
8. Zhang L., Dong L.H., Wang D.S., Fan C.H., Zhou Y. (2012): A survey on electrode materials for electrical discharge machining. *Materials Science Forum*, *697*, 495-499. doi: 10.4028/www.scientific.net/MSF.697-698.495
9. Weidenbaum B., Hoyt E.W., Zimmerman D.L., Cummings W.V., Antony K.C. (1962). Properties of some high temperature control materials, in: Simnad T., Zumawalt L.R. (ed.): *Materials and fuels for high temperature nuclear energy applications*, The M.I.T. Press, Massachusetts, pp. 315-343.
10. Middleburgh S.C., Parfitt D.C., Blair P.R., Grimesw R.W. (2011): Atomic Scale Modeling of Point Defects in Zirconium Diboride. *Journal of the American Ceramic Society, 94*, 2225–2229. doi:10.1111/j.1551-2916.2010.04360.x
11. Sonber J.K., Suri A.K. Synthesis and consolidation of zirconium diboride: review. *Advances in Applied Ceramics*, *110*(6), 321-334. doi: 10.1179/1743676111Y.0000000008
12. Sonber J.K., Murthy T.S.R.Ch., Subramanian C., Hubli R.C., Suri A.K. (2013). Novel processing methods for Ultra High Temperature Ceramics, in: *MAX Phase and Ultra-High Temperature Ceramics for Extreme Environments*. IGI Global, ISBN: 9781466640665.
13. Sonber J.K., Murthy T.S.R.Ch., Subramanian C., Hubli R.C., Fotedar R.K., Suri A.K. (2014): Effect of WSi_2 addition on densification and properties of ZrB_2. *Advances in Applied Ceramics*, *113*, 114-119. doi:10.1179/1743676113Y.0000000125
14. Sonber J.K., Murthy T.S.R.Ch., Subramanian C., Hubli R.C., Suri A.K. (2012): Effect of EuB_6 addition on densification and properties of ZrB_2. *International Journal of Refractory Metals and Hard Materials*, *35*, 96-101. doi:10.1016/j.ijrmhm.2012.04.012
15. Sonber J.K., Murthy .S.R.Ch., Subramanian C., Krishna-murthy N., Hubli R.C., Suri A.K. (2012): Effect of $CrSi_2$ and HfB_2 addition on densification and properties of ZrB_2. *International Journal of Refractory Metals and Hard Materials*, *31*, 125-131. doi:10.1016/j.ijrmhm.2011.10.001
16. Zhu S., Fahrenholtz W.G., Hilmas G.E., Zhang S.C. (2007): Pressureless sintering of carbon-coated zirconium diboride powders. *Materials Science and Engineering: A*, *459*(1), 167-171. doi:10.1016/j.msea.2007.02.116
17. Mishra S.K., Das S.K. (2005): Sintering and microstructural behaviour of SHS produced zirconium diboride powder with the addition of C and TiC. *Materials Letter*s, *59*(27), 3467-3470. doi:10.1016/j.matlet.2005.06.015
18. Mishra S.K., Pathak L.C. (2008): Effect of carbon and titaniumcarbide on sintering behaviour of zirconium diboride. *Journal of Alloys and Compounds*, *465*(1), 547-555. doi:10.1016/j.jallcom.2007.11.004
19. Monteverde F., Bellosi A., Guicciardi S. (2002): Processing and properties of zirconium diboride-based composites. *Journal of the European Ceramic Society, 22*, 279–288. doi:10.1016/S0955-2219(01)00284-9
20. Rezaie A., Fahrenholtz W.G., Hilmas G.E. (2007): Effect of hot pressing time and temperature on the microstructure and mechanical properties of ZrB_2–SiC. *Journal of Materials Science*, *42*(8), 2735-2744. doi:10.1007/s10853-006-1274-2
21. Li C.W., Lin Y.M., Wang M.F., Wang C.A. (2010): Preparation and mechanical properties of ZrB_2-based ceramics using $MoSi_2$ as sintering aids. *Frontiers of Mate-rials Science in* China, *4*(3), 271-275. doi:10.1007/s11706-010-0084-2
22. Wang M., Wang C.A., Zhang X. (2012): Effects of SiC platelet and $ZrSi_2$ additive on sintering and mechanical properties of ZrB_2-based ceramics by hot-pressing. *Mate-rials & Design*, *34*, 293–297. doi:10.1016/j.matdes.2011. 08.016
23. Silvestroni L., Sciti D. (2011): Densification of ZrB_2-$TaSi_2$ and HfB_2-$TaSi_2$ ultra-high-temperature ceramic composites. *Journal of the American Ceramic Society*, *94*(6), 1920-1930. doi:10.1111/j.1551-2916.2010.04317.x
24. Sonber J.K., Murthy .S.R.Ch., Subramanian C., Kumar S., Fotedar R.K., Suri A.K. (2011): Investigations on synthesis of ZrB_2 and development of new composites with HfB_2 and $TiSi_2$. *International Journal of Refractory Metals and Hard Materials, 29*(1), 21-30. doi:10.1016/j.ijrmhm.2010.06.007
25. Anstis G.R., Chantikul P., Lawn B.R., Marshall D.B. (1981): A critical evaluation of indentation techniques for measuring fracture toughness: I, direct crack measurements. *Journal of the American Ceramic Society*, *64*, 533–538. doi:10.1111/j.1151-2916.1981.tb10320.x
26. Guo W.M., Vleugels J., Zhang G.J., Wang P.L., Biest O.V. (2009): Effects of Re_2O_3 (Re = La, Nd, Y and Yb) addition in hot-pressed ZrB_2–SiC ceramics. *Journal of the European Ceramic Society, 29*, 3063–3068. doi:10.1016/j.jeurceramsoc.2009.04.021
27. Wang H., Chen D., Wang C.N., Zhang R., Fang D. (2009): Preparation and characterization of high-toughness ZrB_2 /Mo composites by hot pressing process. *International Journal of Refractory Metals and Hard Materials*, *27*(6), 1024-1026. doi:10.1016/j.ijrmhm.2009.06.003
28. Zhu T., Xu L., Zhang X., Han W., Hu P., Weng L. (2009): Densification, microstructure and mechanical properties of ZrB_2–SiC_w ceramic composites. *Journal of the European Ceramic Society*; *29*, 2893–2901. doi:10.1016/j.jeurceramsoc.2009.03.008
29. Chamberlain A.L., Fahrenholtz W.G., Hilmas G.E. (2004): High strength zirconium diboride based ceramics. *Journal of the American Ceramic Society*, *87*(6), 1170-1172. doi: 10.1111/j.1551-2916.2004.01170.x
30. Silvestroni, L., Sciti, D. (2014): TEM analysis, mechanical characterization and oxidation resistance of a highly refractory ZrB2 composite. *Journal of Alloys and Com-pounds*, *602*, 346-355. doi:10.1016/j.jallcom.2014.02.133
31. Ran S., Sun H., Vanmeensel K., Huang S., Vleugels J. (2014): Influence of ZrH_2 addition on pulsed electric current sintered ZrB_2-SiC composites, *Scripta Materialia*, *77*, 41-44. doi:10.1016/j.scriptamat.2014.01.014
32. Sciti D., Brach M., Bellosi A. (2005): Oxidation behavior of a pressureless sintered ZrB_2-$MoSi_2$ ceramic composite. *Journal of Materials Research*, *20*(4), 922-930. doi:10.1557JMR.2005.0111
33. Peng F., Speyer R.F. (2008): Oxidation resistance of fully dense ZrB_2 with SiC, TaB_2, and $TaSi_2$ additives. *Journal of the American Ceramic Society*, *91*(5), 1489-1494. doi:10.1111/j.1551-2916.2008.02368.x
34. Dehdashti M.K., Fahrenholtz W.G., Hilmas G.E. (2014): Effects of temperature and the incorporation of W on the oxidation of ZrB_2 ceramics. *Corrosion Science*, *80*, 221-228. doi:10.1016/j.corsci.2013.11.030
34. Zhao J., Liu H.T., Liu J.X., Zhang G.J. (2014): ZrB_2 ceramics doped with AlB_2. *Ceramics International*, *40*(6), 8915-8920. doi:10.1016/j.ceramint.2014.01.037